

Study on Photodegradation of 4,4'-Dibromobiphenyl by TiO₂ Films

PING ZHANG*[†], CAIHONG JI and PINGFANG HAN

College of Chemistry and Chemical Engineering,

Nanjing University of Technology, Nanjing 210009, P.R. China

Fax: (86)(518)85985010; Tel: (86)(518)82786057; E-mail: lygzhangping@hotmail.com

The TiO₂ film photodegradation of 4,4'-dibromobiphenyl (4,4'-DBB) have been investigated by employing a UV lamp (8 W). Hydrogen peroxide and initial 4,4'-DBB concentrations, initial pH and possible reaction intermediates were also determined. The mechanism of photocatalytic degradation of 4,4'-DBB by TiO₂ thin film was discussed. The dynamics of photocatalytic degradation of 4,4'-DBB was also studied. The results indicate that the 4,4'-DBB degradation rate decreased with the increase of initial 4,4'-DBB concentration under the same conditions. The degradation rate of 0.5 g/L 4,4'-DBB was 90 % within 4 h. In contrast to the results of the studies on other organic compounds, the optimum pH for degradation of 4,4'-DBB was 11. The removal efficiency was higher under alkaline conditions than acidic conditions. The principal products of 4,4'-DBB decomposition was 4-monobromobiphenyl, biphenyl and benzene derivatives. The reaction of photocatalytic degradation of 4,4'-DBB by TiO₂ thin film followed a pseudo first-order kinetics, the reaction rate constant also decreased with the increase of initial 4,4'-DBB concentration.

Key Words: 4,4'-Dibromobiphenyl, TiO₂ thin film, Photodegradation.

INTRODUCTION

Polybrominated biphenyls (PBBs) have been widely used as flame retardants in plastics, carpets, electronic equipment, textiles and building materials around the world because of their physicochemical properties¹. The chemical and thermal stabilities that made PBBs useful have also created serious environmental problems². The study of PBBs has been of considerable interest because of their environmental toxicity.

In recent years, our research group have studied many ways to deal with wastewater contains PBBs. We studied the degradation effect of 4,4'-DBB by Fenton's reagent, when the mol ratio of H₂O₂/Fe²⁺ was 10:1, pH value was 1.4-2.4, the remove efficiency was up to 99 %³. Ozone (O₃) alone and O₃/H₂O₂ were also studied to degrade 4,4'-DBB, the final removal rate reached 78.0 %⁴. Other methods like O₃/US, photosensitive of oxidation, have made some progresses^{5,6}. But there are still some problems, such as excessive amount of oxidants, high cost of degradation, *etc.*

[†]Lianyungang Technical College, Lianyungang 222006, P.R. China.

It is well established that titanium dioxide (TiO_2) is the best candidate for photocatalytic applications: non-toxic, chemically stable, tunable due to size effects, *etc.* Photocatalytic oxidation (PCO) uses a semiconductor as a photocatalyst to capture light energy and produce the high oxidizing hydroxyl radical (OH^\bullet) to degrade various compounds. The advantage of photocatalytic oxidation over other treatment methods is its high efficiency and non-selectivity. In addition, the TiO_2 film can be separated from the treatment stream and reused⁷.

This study was designed to get detailed informations about the TiO_2 photo-destruction mechanisms of PBBs. We initiated a systematic study of the TiO_2 photodegradation of 4,4'-dibromobiphenyl (4,4'-DBB). In addition, the optimal physico-chemical conditions, including initial 4,4'-DBB concentration, hydrogen peroxide concentration and pH of the reaction solution were also determined.

EXPERIMENTAL

4,4'-Dibromobiphenyl (4,4'-DBB, AR), reagent grade titanium(IV) butoxide [$\text{Ti}(\text{O}-n\text{C}_4\text{H}_9)_4$, abbreviated as TBOT], absolute ethanol ($\text{C}_2\text{H}_5\text{OH}$, AR), triethanolamine ($\text{N}(\text{C}_2\text{H}_5\text{O})_3$, AR), hydrogen peroxide (H_2O_2 , 30 wt. %).

UV lamp (254 nm, 8 W), GC-MS (Trace-DSQ) purchased from American Thermo Finnigan company, XRD diffraction measurements purchased from Germany Bruker company, GC (sp-6800A).

Preparation of TiO_2 thin films: $\text{Ti}(\text{O}-n\text{C}_4\text{H}_9)_4$ was first mixed with $\text{N}(\text{C}_2\text{H}_5\text{O})_3$ and a small amount of $\text{C}_2\text{H}_5\text{OH}$ under vigorous stirring (*ca.* 1450 rpm) in air at room temperature for 1 h. Then a mixture of ethanol and deionized water was poured. The favourable $\text{Ti}(\text{O}-n\text{C}_4\text{H}_9)_4:\text{N}(\text{C}_2\text{H}_5\text{O})_3:\text{C}_2\text{H}_5\text{OH}:\text{deionized water}$ mol composition was found to be 1:1:26.5:1. The reaction was allowed for 2 h, then the homogeneous and transparent solution was obtained. The resultant sol was stable for a period of 7 days followed by the occurrence of gelation. Complete drying of the gel thus obtained under ambient conditions caused shrinkage of the network resulting into the xerogels⁸.

The glass substrate ($76.2 \times 25.4 \text{ mm}^2$) was used as the conducting supporting materials for TiO_2 . The glass was cleaned with acetone in an ultrasonic bath for 15 min. The glass was dried in an oven at 100°C for 15 min and then dip-coated with sol-gel solution and left to dry at room temperature⁹. The coated glass was heated at 100°C for 0.5 h. Then, the plate was annealed at 500°C in a furnace for 2 h. Finally the plate was cooled in the furnace at room temperature. This step was repeated several times until the plate had desired layers.

Experiments of TiO_2 film photocatalytic degradation of 4,4'-DBB: The reaction was carried out in a 250 mL glass reactor. The TiO_2 thin film was put in the reactor containing 50 mL aqueous 4,4'-DBB (ethanol as cosolvent). The reaction mixture was exposed to the UV lamp perpendicularly and the distance between the lamp and the aqueous surface was kept within 8 cm. A stainless steel cylinder covered the whole reactor to prevent the escape of UV light. All operations were conducted

at ambient temperature. After irradiating the solution for a definite time, the concentration of 4,4'-DBB was measured by using UV-visible (UV-Vis) spectroscopy and a gas chromatograph. Photocatalytic oxidation degradation intermediates/product(s) were determined using gas chromatography-mass spectrometry.

Determination of 4,4'-DBB concentration: A gas chromatograph coupled with a hydrogen flame ionization detector (GC-FID), sp-6800A GC system, was used to measure the concentration of 4,4'-DBB. Nitrogen gas was used as carrier gas¹⁰. The hydrogen flame ionization detector (FID) was maintained at 320 °C. The GC column was a capillary column (SE 30). The column temperatures were 270 °C, the temperature of injector was 320 °C. The concentration of 4,4'-DBB was detected using internal standard method. Photocatalytic oxidation efficiency expressed as removal efficiency (RE in %) calculated by the following equation:

$$f_i' = m_i \times A_s / (m_s \times A_i)$$

$$p_i = \frac{A_i}{A_s} \times f_i' \times \frac{m_s}{m} \times 100 \%$$

$$RE = \frac{p_{i1} - p_{i2}}{p_{i1}} \times 100 \%$$

where A_i and A_s are the peak areas of tetra-CB before and after photocatalytic oxidation treatment.

X-ray diffraction measurements were carried out with a custom-built diffractometer equipped with graphite monochromator and analyzer crystal sizes were determined based on the anatase (101) and (200) peaks using the Scherrer formula.

RESULTS AND DISCUSSION

XRD analysis of TiO₂ films: The XRD patterns were determined by X-ray powder diffraction measurements using Ni-filtered CuK_α radiation in the range of 2θ from 10 to 50° for confirming the crystal phases of heat-treated TiO₂ films. Fig. 1 shows the XRD patterns of the films with different layers. It can be seen that there is no crystalline phase observed in one layer. As the layer is increased up to two or above, a clear signal of the diffraction peaks at 2θ = 25.3° and 48.10° starts to appear¹¹, the intensity of these diffraction peaks increases with the increase of the layer. The film showed⁸ the peaks characteristic of the anatase phase at 2θ = 25.3° and 48.10 (CuK_α) oriented along (101) and (200) planes, respectively.

It should be stressed here that all peaks observed can be assigned to specific lattice planes of the anatase phase of TiO₂, which corresponds to JCPDS Patterns No. 21-1272. These XRD results demonstrate that nanocrystalline anatase TiO₂ sol-gel thin films can be obtained when a heat treatment temperature is at 500 °C. The crystallite size of the (101) plane from the films shown in Fig. 1 was determined from the Scherrer formula. The crystallite size of TiO₂ thin films can be deduced from XRD line broadening using the Scherrer equation. $L = K\lambda/\beta \cos \theta$.

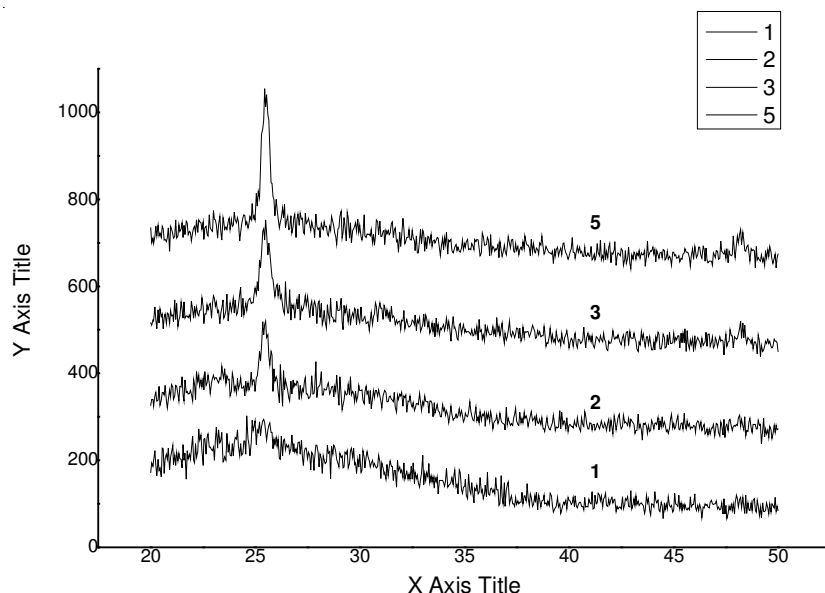


Fig. 1. XRD patterns of TiO₂ films with different thickness

Where L is the crystallite size of TiO₂ thin films, K is a constant (0.94), λ is the wavelength of X-ray ($\text{CuK}\alpha = 1.54056 \text{ \AA}$), β is the true half-peak width and θ is the half diffraction angle of the centroid of the peak in degree. Any contributions to broadening due to the nonuniform stress were neglected and the instrumental line width in the XRD apparatus was subtracted¹². The crystallite size of anatase TiO₂ increased from 15 to 22 nm.

Effect of TiO₂ UV photocatalytic: Fig. 2 shows the degradation of 2 g/L of 4,4'-DBB by TiO₂/UV photocatalytic and UV alone, the intensity of the UV lamp was 224 mW/cm². It can be observed from Fig. 2 that the removal efficiency of 4,4'-DBB was increased with the time extend. Both TiO₂/UV photocatalytic and UV light had its potential to degrade 4,4'-DBB as described above and that the degradation rate under TiO₂ photocatalytic higher than that under UV alone.

Since light absorption is a prerequisite for photodegradation, UV-visible absorption spectra of 4,4'-DBB were obtained in Fig. 3. All of them show a strong absorption band in the range of 220-310 nm (k wave band), which arises from aromatic $\delta\text{f}-\delta^*$ transition. The band became wider because Br- taken off from 4,4'-DBB and the intermediates products may be biphenyl. As the number of substituted bromines increases in solution, the absorption band shifts to longer wavelengths. The nonbonding electrons on Br atoms interact with the δ electrons of the aromatic ring, which apparently stabilizes the δ^* state with a little red shift. The weak absorption band extending over 200-220 nm (R wave band) is ascribed to $\text{nf}-\delta^*$ transition. So we can say the degradation of 4,4'-DBB was a process of debromination step by step.

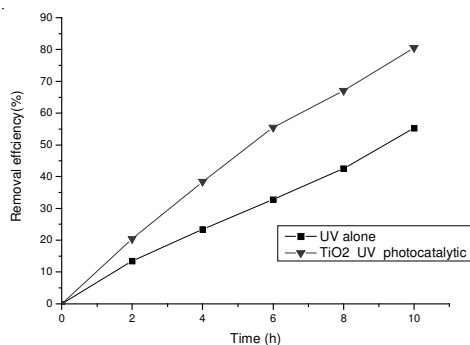


Fig. 2. Effect of TiO₂/UV and UV on the degradation ratio

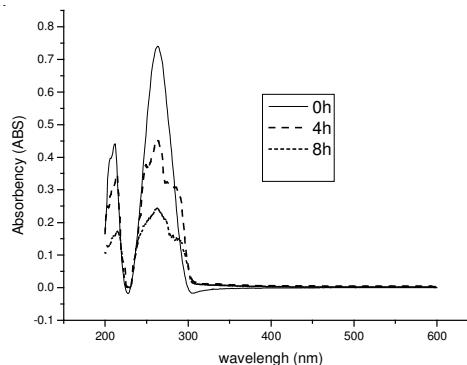


Fig. 3. UV spectrogram of 2 g/L 4,4'-DBB degradation after 4 and 8 h

Effect of 4,4'-DBB initial concentration: Fig. 4 shows the effect of initial 4,4'-DBB concentration was 0.5, 1.0, 1.5 and 2 g/L, respectively on degradation. The degradation rate decreased with the increase of initial 4,4'-DBB concentration under the same conditions. After 8 h degradation, the according removal efficiency was 96.9, 82.1, 69.33 and 52.92 %, respectively. But the according total degraded mass was 0.484, 0.821, 1.039 and 1.058 g, so that the total degraded mass increased with the increase of initial 4,4'-DBB concentration. The initial 4,4'-DBB concentration of 0.5 g/L was completely degraded within 4 h.

Effect of H₂O₂ volume: Hydrogen peroxide was added to enhance production of OH[•] through a series of redox reactions under the assumption that H₂O₂ can enhance the removal of 4,4'-DBB. As the H₂O₂ volume increased from 0 to 7 mL, the 4,4'-DBB degradation did increase (Fig. 5). However, H₂O₂ is a OH[•] scavenger, so the excess H₂O₂, OH[•] produced was quenched by the H₂O₂ rather than reacting with the 4,4'-DBB. Moreover, as the rate of OH[•] generation increased, the reaction between OH[•] became faster, even faster than the rate of oxidation of the organic pollutants by OH[•]. As a result, the OH[•] were quenched by themselves and not available to oxidize the organic pollutants¹³.

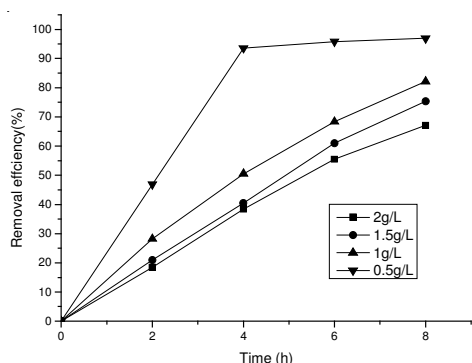


Fig. 4. Effect of initial 4,4'-DBB concentration on the degradation ratio

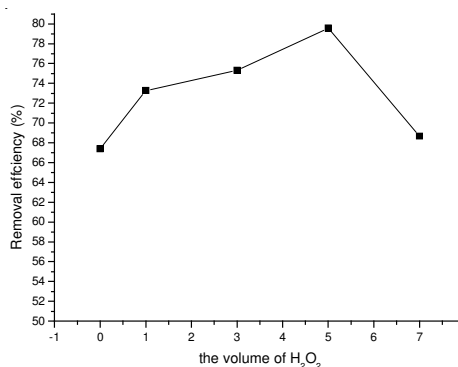


Fig. 5. Effect of H₂O₂ volume on 4,4'-DBB removal efficiency

Effect of initial pH: Under alkaline conditions and acidic conditions, the 4,4'-DBB degradation ratio was higher than neutral condition. Results from these other studies suggested that OH^\bullet was generated mainly from the oxidation of water by the positive hole (h^+) at lower pH levels, while the electron reduction of oxygen (dissolved oxygen, DO) was the dominant reaction at higher pH levels¹⁴. Since the photocatalytic oxidation reaction was not aerated in this study, the DO level was relatively low (Fig. 6). Thus, at high pH levels, the production of the removal efficiency was higher under alkaline conditions than acidic conditions.

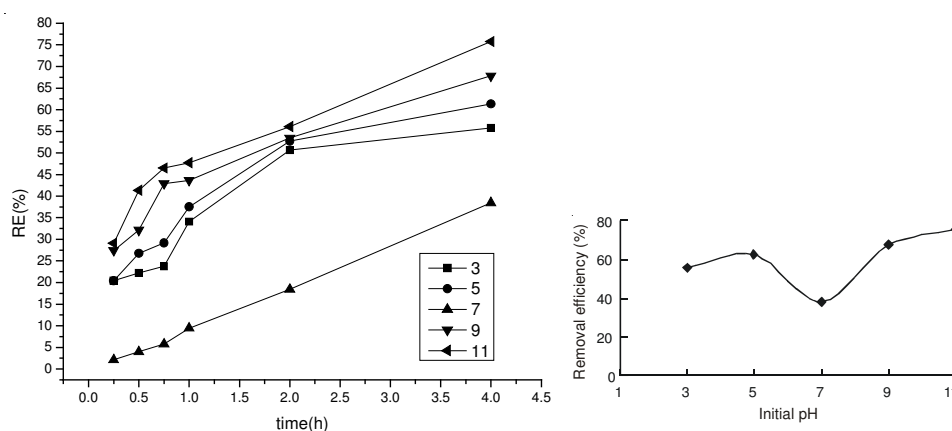


Fig. 6. Effect of initial pH on the degradation ratio

The pH influenced not only the surface characteristics of TiO_2 , but also the dissociation of 4,4'-DBB and the formation of the OH^\bullet radical. Hence, the effects of pH on the efficiency of degradation are difficult to interpret. The surface of the TiO_2 was charged positively at $\text{pH} < \text{pH}_{\text{zpc}}$ and TiOH^{2+} dominated. Conversely, the predominant species was TiO^- at $\text{pH} > \text{pH}_{\text{zpc}}$ ^{15,16}. 4,4'-Dibromobiphenyl is mainly in the molecular form ($\text{C}_{12}\text{H}_8\text{Br}^-$). Since the TiO_2 was 6.5, electrostatic interactions between the TiO_2 surface and the $\text{C}_{12}\text{H}_8\text{Br}^-$ resulted in adsorption at high pH, accelerating decomposition. Therefore, the reaction rates were higher in alkaline than under neutral or acidic conditions. Various reaction mechanisms, including the attack by OH^\bullet radicals, direct oxidation by positive holes and direct reduction by electrons are responsible for the photodegradation of organic compounds. Accordingly, the effect of pH on photodegradation efficiency differed from those associated with photocatalysts and parent compounds.

TiO_2 UV photocatalytic degradation kinetics: The photodegradation of 4,4'-DBB followed the Langmuir-Hinshelwood mechanism and for diluted solutions, reaction was of first order: $\ln c/c_0 = kt$, where c_0 [g/L] is the initial concentration of 4,4'-DBB, c [g/L] is the concentration measured at the interval of time, t [min] and k [min^{-1}] is the apparent photodegradation rate constant. It should be noted that the slope of decay ($\ln c/c_0$) appeared in a good agreement with pseudo-first order kinetics

(Fig. 7). The kinetic constants (k , min^{-1}) and the corresponding correlation coefficients (R) are calculated and listed in Table-1. The reaction rate constant also decreased with the increase of initial 4,4'-DBB concentration.

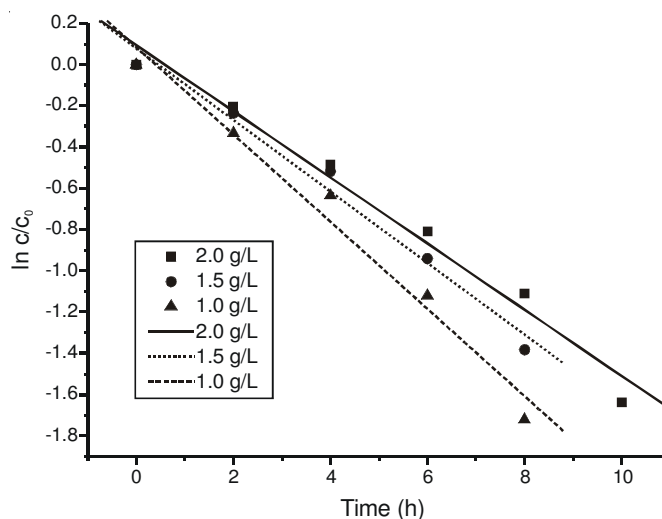


Fig. 7. Pseudo-first-order decay curves of 4,4'-DBB

TABLE-1
REACTION RATE CONSTANTS OF 4,4'-DIBROMOBIPHENYL AT
DIFFERENT INITIAL CONCENTRATION

Concentration (g/L)	k	R	SD	P
2.0	0.16039	0.98922	0.09931	1.73578 E-4
1.5	0.17350	0.99079	0.08660	0.00106
1.0	0.21149	0.98899	0.11553	0.00138

Conclusion

Anatase TiO₂ thin film photocatalysts were successfully prepared by using sol-gel. The XRD studies revealed the nanocrystalline nature of the films was anatase when heat treated at 500 °C. In photolysis, 0.5 g/L 4,4'-DBB was degraded more than 90 % with an exposure time to UV light for 4 h. The optimum pH for degradation of 4,4'-DBB was 11. The removal efficiency was higher under alkaline conditions than acidic conditions. The presence of excess H₂O₂ will reduce the 4,4'-DBB degradation, probably due to inhibition in the production of OH[•], the major oxidizing species in the photocatalytic oxidation process.

ACKNOWLEDGEMENTS

The authors gratefully acknowledge the financial support of this work by Qinglan Project Foundation of Jiangsu Province and Industry Promotion Project of Jiangsu Province (JHZD08-49).

REFERENCES

1. X. Sh. Miao, Sh. G. Chu and X.B. Xu, *Chemosphere*, **39**, 1639 (1999).
2. Q.D. Huang and C.S. Hong, *Chemosphere*, **41**, 871 (2000).
3. L. Wang, H.X. Wang and X.P. Lu, *Environ. Sci. Technol.*, **12**, 69 (2007).
4. L. Wang, Y.J. Zhu and X.P. Lu, *J. Nanjing Univ. Technol.*, **29**, 102 (2007).
5. B. Schreiber and M. Dupeyrata, *J. Electroanal. Chem.*, **104**, 427 (1979).
6. C.H. Ji, P. Zhang and P.F. Han, *Chin. J. Environ. Eng.*, **3**, 6 (2009).
7. Y.D. Jaoued, M. Thibodeau, J. Robichaud, S. Balaji, S. Priya, N. Tchoukanova and S.S. Bates, *J. Photochem. Photobiol. A: Chem.*, **193**, 271 (2008).
8. A. Verma, S.B. Samanta, A.K. Bakhshi and S.A. Agnihotri, *Solar Energy Mater. Solar Cells*, **88**, 47 (2005).
9. I. Truijen, M.K. Van Bael and H. Mullens, *J. Sol-Gel Sci. Technol.*, **37**, 19 (2006).
10. H.X. Zhao, Q. Zhang and X.Y. Xue, *Anal. Bioanal. Chem.*, **382**, 1304 (2005).
11. W.X. Que, A. Uddin and X. Hu, *J. Power Sources*, **159**, 353 (2006).
12. I. Truijen, M.K. Van Bael, H. Van den Rul, J. D'Haen and J. Mullens, *J. Sol-Gel Sci. Technol.*, **41**, 43 (2007).
13. K.H. Wong, S. Tao, R. Dawson and P. K. Wong, *J. Hazard. Mater.*, **109**, 149 (2004).
14. L. Andronic and A. Duta, *Thin. Solid Films*, **515**, 6294 (2007).
15. P. Fernandez-Ibanez, J. Blanco, S. Malato and F.J. de las Nieves, *Water Res.*, **37**, 3180 (2003).
16. A. Fernandez-Nieves and F.J. de las Nieves, *Colloids Surf. A: Physicochem. Eng. Aspects*, **148**, 231 (1999).

(Received: 10 August 2009; Accepted: 21 January 2010) AJC-8343

**THE 3RD INTERNATIONAL SYMPOSIUM ON ORGANIC AND
INORGANIC ELECTRONIC MATERIALS AND RELATED
NANOTECHNOLOGIES (EM-NANO 2010)**

22 — 25 JUNE 2010

TOYAMA, JAPAN

Contact:

Prof. Hiroyuki Okada,
Graduate School of Science and Engineering for Research,
University of Toyama, 3190 Gofuku, Toyama 930-8555, Japan
Tel: +81-76-445-6730, Fax: +81-76-445-6732,
E-mail: emabst@eng.u-toyama.ac.jp,
Web site: <http://www3.u-toyama.ac.jp/emnano/>